

Review

Kinetics of Ions in Post-Lithium Batteries

Efstratia N. Sgourou ¹, Aspasia Daskalopulu ² , Lefteri H. Tsoukalas ³, Ioannis L. Goulatis ², Ruslan V. Vovk ⁴
and Alexander Chroneos ^{2,5,*} 

¹ Solid State Physics Section, University of Athens, Panepistimiopolis Zografos, 15784 Athens, Greece; e_sgourou@hotmail.com

² Department of Electrical and Computer Engineering, University of Thessaly, 38333 Volos, Greece; aspasia@uth.gr (A.D.); yannislgoul@gmail.com (I.L.G.)

³ School of Nuclear Engineering, Purdue University, West Lafayette, IN 47906, USA; tsoukala@purdue.edu

⁴ Department of Physics, V. N. Karazin Kharkiv National University, 4 Svobody sq., 61077 Kharkiv, Ukraine; rvvovk2017@gmail.com

⁵ Department of Materials, Imperial College London, London SW7 2BP, UK

* Correspondence: alexander.chroneos@imperial.ac.uk; Tel.: +30-697-877-5320

Abstract: There is a technological necessity for more efficient, abundant, and sustainable materials for energy storage applications. Lithium-ion batteries dominate, however, there are a number of sustainability, economic, and availability issues that require the investigation of post-lithium batteries. In essence, the drive is to move to non-lithium-containing batteries as there is simply not enough lithium available to satisfy demand in a few years. To find alternative ions migrating at appropriate rates in crystal lattices requires significant research efforts and, in that respect, computational modeling can accelerate progress. The review considers recent mainly theoretical results highlighting the kinetics of ions in post-lithium oxides. It is proposed that there is a need for chemistries and ionic species that are sustainable and abundant and in that respect sodium, magnesium, and oxygen ion conduction in batteries is preferable to lithium. The limitations and promise of these systems are discussed in view of applications.

Keywords: batteries; diffusion; defect engineering; solid oxide fuel cells; nuclear materials; oxygen battery; heterointerfaces; doping; sodium; magnesium



Citation: Sgourou, E.N.;

Daskalopulu, A.; Tsoukalas, L.H.;

Goulatis, I.L.; Vovk, R.V.; Chroneos,

A. Kinetics of Ions in Post-Lithium Batteries. *Appl. Sci.* **2023**, *13*, 9619.

<https://doi.org/10.3390/app13179619>

Academic Editor: Minas M. Stylianakis

Received: 1 August 2023

Revised: 19 August 2023

Accepted: 24 August 2023

Published: 25 August 2023



Copyright: © 2023 by the authors. Licensee MDPI, Basel, Switzerland. This article is an open access article distributed under the terms and conditions of the Creative Commons Attribution (CC BY) license (<https://creativecommons.org/licenses/by/4.0/>).

1. Introduction

The growing need for electricity generation and storage has led to a plethora of techniques seeking better energy materials to meet growing needs in technological applications that include, but are not limited to, electric vehicles, grid electricity storage, electronic products, energy harvesting, and nanoelectronics [1–25]. Lithium compounds such as lithium carbonate (Li₂CO₃), lithium oxide (Li₂O), and lithium hydroxide (LiOH) offer favorable electrochemical fundamentals and cost-effective manufacturing options for the fabrication of rechargeable batteries, which utilizes approximately three-quarters of the global production of lithium at present. In recent years, the explosive demand for lithium is raising questions of sustainability mostly due to rather limited known global reserves and regional concentration. Nearly half of the world's known economically recoverable reserves of 105 million tonnes are concentrated in Bolivia, Chile, and Argentina (the so-called *lithium triangle*) while nearly half of the annual production of lithium is currently taking place in Australia. On the demand, side there are doubts as to whether there is enough lithium to move into electricity for the nearly 1.5 billion cars on the planet, let alone provide for grid storage and non-transportation applications. Although there seems to be sufficient lithium to enable, at least the early stages of, the green transition and Net Zero by 2050, numerous environmental, supply chain, and sustainability challenges, motivate, with a sense of urgency, scientific research and development in post-lithium energy storage technologies.

The novel materials considered for post-lithium energy storage have typically exotic crystallography and are composed of substances that are not abundant or sustainable considering the massive scale required for technological solutions to make a real difference [26–50]. Here, we consider three paradigms in energy storage applications, such as sodium (Na), divalent conductors (magnesium (Mg)), and finally oxygen (O), which have been proposed as alternatives to Li-ion conductors.

The drive to substitute Li ions is due to its high price and the limited lithium resources [43]. Sodium in comparison is more than four orders of magnitude more abundant in the Earth's crust and also in seawater, whereas the working principle of Na-ion batteries is similar to Li-ion batteries [43]. The technological issues in Na-ion battery materials include slow insertion/extraction kinetics and low theoretical capacity and these can be traced to the larger size of the sodium ion as compared to the lithium ion. The crystal structure is the matrix where the ions migrate and the community is trying to assess which crystal structures will provide the necessary kinetics for Na ion that will compensate for its larger size as compared to Li ion.

Magnesium-based rechargeable batteries are currently being considered by the community as potential candidates for the next generation energy storage because of their high gravimetric and volumetric capacity, non-toxicity, abundance, and higher melting temperature [44,45]. Importantly, the ionic size of the Mg^{2+} ion is comparable to the Li^+ ion, however, the stronger ionic interaction of Mg^{2+} ions in the lattice will make intercalation harder [44,45]. These issues can be rectified by reducing the size of the cathode ions in the crystal and by increasing the shielding of Mg^{2+} [33,34].

The first part of this review briefly discusses the computational methods to model oxides. In this part, molecular dynamics (MD) and density functional theory (DFT) are discussed. The second part of the review is focused on recent efforts to substitute lithium ions for energy storage applications. Sodium and magnesium-containing oxides are considered and the focus is on the ionic diffusion properties. Thereafter, we discuss oxygen ion diffusion and the novel concept of oxygen ion batteries. Then we consider ways to tune ionic diffusion as sodium and magnesium ion-containing materials are lagging behind in the kinetics as compared with lithium materials. Finally, perspectives and the future outlook are given.

2. Materials and Methods

Molecular Dynamics and Density Functional Theory

In this review, most of the results are from papers based on MD and DFT. For completeness, we will briefly summarize key aspects of these methods. For more detailed descriptions there are more comprehensive reviews on the computational modeling of inorganic materials [51–53].

The quantum mechanical formulation is the most complete description of nature. In practical terms, however, the analytic solution of the Schrödinger equation for a large number of electrons is computationally intensive and intractable mainly because of the complexity of many electron interactions [54]. In an effort to overcome these problems, the DFT approach was developed [55–57]. In the DFT approach, the exchange-correlation energy of electrons is described by the local density approximation (LDA) or the generalized gradient approximation (GGA) or with the more appropriate and rigorous hybrid functionals that include a part of exact exchange from the Hartree–Fock theory [57]. The main idea is the use of a plane-wave basis set with the pseudopotential method so that the core electrons are described by effective potentials, whereas the valence electrons can evolve explicitly. Typically, in DFT the activation energy of ionic diffusion can be predicted by identifying the minimum energy path (for example using the nudged elastic band method) [58]. Although the DFT approach is a simplification and renders the derivation of results tractable, whereas analytical approaches would not, the simulation size is still limited (typically hundreds of atoms). Therefore, the use of this approach to more extended problems (i.e., microstructures or extended defects) is not possible.

An alternative way that is popular when studying diffusion in oxides (or more extended defects such as grain boundaries) is classical potential-based MD. In classical MD the state of the system can be described by considering the positions and the momenta of all the particles with Newton's equations of motion being solved iteratively to predict the evolution of the system. The interactions between particles are through potential energy functions and for ionic systems this is within the classical Born-like description [59]. Typically, the ionic interactions can be modeled by a Coulombic term (long-range) and by a short-range parameterized pair potential [60–62]. The computational simplicity of MD allows the consideration of very extended systems (millions of ions), however, they cannot describe the electronic structure of the system. Nevertheless, classical MD is a valuable tool when considering the diffusion and defect chemistry of ionic materials.

Complementary to DFT and MD are thermodynamic models that can aid in the understanding of material properties for a wide range of pressures, temperatures [63–75], and methods such as cluster expansion and special quasirandom structures that can be used to render the compositional and structural complexity of solid solutions computationally tractable [76–88]. These have become increasingly important in the past years as it is becoming common to investigate systems with ever-increasing structural complexity. In this, it is hard to randomly select one or a few “representative” structure(s) to perform the atomic scale investigation, whereas it is practically impossible to investigate all possible configurations, particularly for extended systems. In that respect, the special quasirandom structures method can offer designed smaller cells that are representative of the local structures of solid solutions. That is, it is not required to do thousands of calculations in many extended supercells, but rather a few hundred (typically) calculations in a single cell that captures all the important local environments [77,78,82–88]. Combining computational techniques with experiments (refer for example in [13,25] and references therein) or advanced methods such as neural networks [35] is the way forward.

3. Post-Lithium Ionic Conductors

3.1. Sodium-Ion Batteries

Sodium (Na) is being actively considered as an alternative ion for energy storage applications [44,48,89–105]. In previous studies, we considered a number of sodium-based materials including $\text{NaZr}_2(\text{PO}_4)_3$, $\text{Na}_3\text{Fe}_2(\text{PO}_4)_3$, $\text{Na}_3\text{V}(\text{PO}_4)_2$, NaNiO_2 , NaFeO_2 and $\text{Na}_2\text{MnSiO}_4$. Table 1 reports the activation energies of diffusion of promising Na of candidate Na-ion battery materials, which range from 0.26 to 0.81 eV [41,47,94–97]. It is observed from Table 1 that $\text{NaZr}_2(\text{PO}_4)_3$ (known as NZP- it is NASICON-type) has a very low activation energy of diffusion (0.26 eV) [47]. These static atomistic simulations are in agreement with previous molecular dynamic calculations by Zou et al. [20] that calculated activation energy for Na diffusion of 0.23 eV. Figure 1 is a schematic representation of the long-range Na-ion diffusion and the migration energy profile for the Na pathway in $\text{NaZr}_2(\text{PO}_4)_3$ [47]. DFT simulations indicate that $\text{NaZr}_2(\text{PO}_4)_3$ is a wide-gap semiconductor, however, the exoergic incorporation of sodium leads to Na^+ ions and electrons. Thus, it is an electronically conductive/high-capacity material that can be used as an electrode [47].

Table 1. The activation energies of diffusion of Na in candidate Na-ion battery materials.

Material	Activation Energy/eV	Comments
$\text{NaZr}_2(\text{PO}_4)_3$	0.26	Ref. [47], vacancy mechanism
$\text{Na}_3\text{Fe}_2(\text{PO}_4)_3$	0.45	Ref. [95], vacancy mechanism
$\text{Na}_3\text{V}(\text{PO}_4)_2$	0.59	Ref. [94], vacancy mechanism
NaNiO_2	0.67	Ref. [96], ab-plane
NaFeO_2	0.65–0.67	Ref. [97], vacancy mechanism
$\text{Na}_2\text{MnSiO}_4$	0.81	Ref. [41], vacancy mechanism

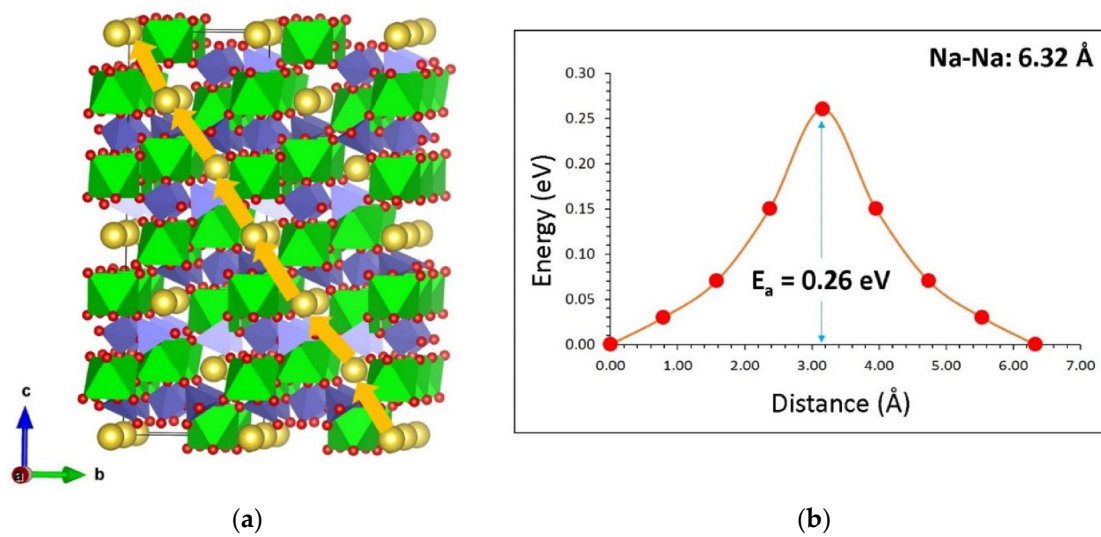


Figure 1. Schematic representation of (a) the long-range Na-ion diffusion and (b) the energy profile for the Na pathway required to migrate via the vacancy mechanism in NaZr₂(PO₄)₃ [47].

Figure 2 is a schematic representation of the crystal structure (space group $C2/c$) and the Na ion diffusion paths calculated in Na₃Fe₂(PO₄)₃. Here the green, purple, and light blue atoms represent the Na ion hopping trajectories [95]. Although there is no experimental work on the diffusion pathways in Na₃Fe₂(PO₄)₃ there are previous atomistic studies on related materials that show the same similar energetics and diffusion mechanisms [30,31]. For example, in the classical atomistic simulation investigation by Clark et al. [31] in Na₂FeP₂O₇, calculated three-dimensional long-range Na ion migration paths in different directions with activation energies for Na self-diffusion 0.33–0.49 eV. Tripathi et al. [30] employed computational modeling to study Na ion diffusion in NaFePO₄ material. They predicted that the lowest energy path is in the [010] direction with an activation energy of only 0.30 eV [30]. Fe-based polyanion materials have reasonably low activation energy for Na-ion diffusion and this suggests that they can be considered for energy storage applications [30,31,95].

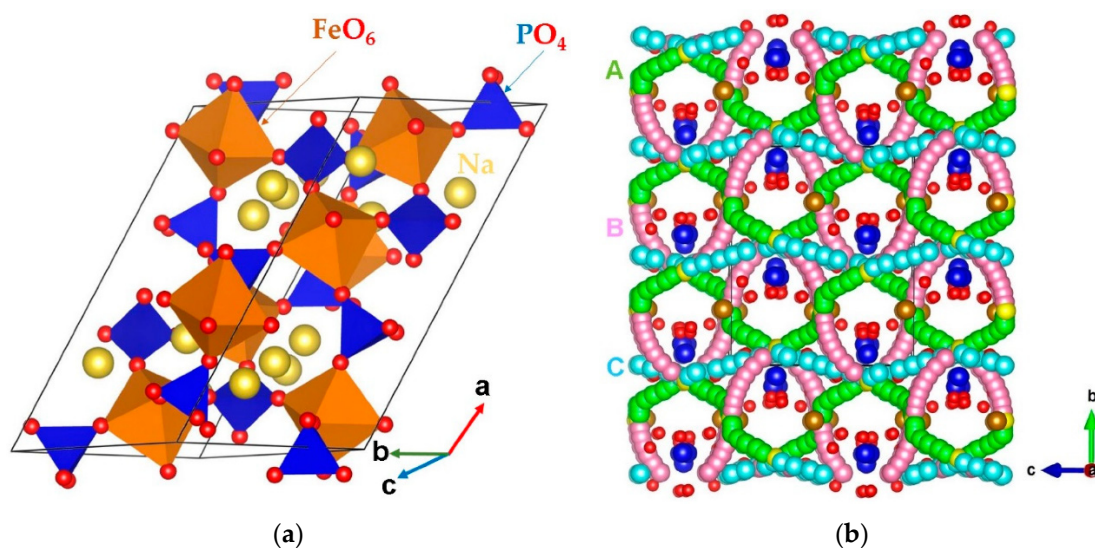


Figure 2. Schematic representation of (a) the crystal structure (space group $C2/c$) and (b) the Na ion diffusion paths (along the bc -plane) calculated in Na₃Fe₂(PO₄)₃. Here, the green, purple, and light blue atoms represent the Na ion hopping trajectories [95].

Figure 3 represents the crystal structure (space group $C2/c$) and the Na ion diffusion paths along the ab -plane in monoclinic $\text{Na}_3\text{V}(\text{PO}_4)_2$ [94]. For $\text{Na}_3\text{V}(\text{PO}_4)_2$ previous calculations are consistent with this two-dimensional Na ion diffusion mechanism [38,94], although there is a range of the calculated activation energies (0.433 eV (DFT) [38] and 0.59 eV (static atomistic simulation) [94]).

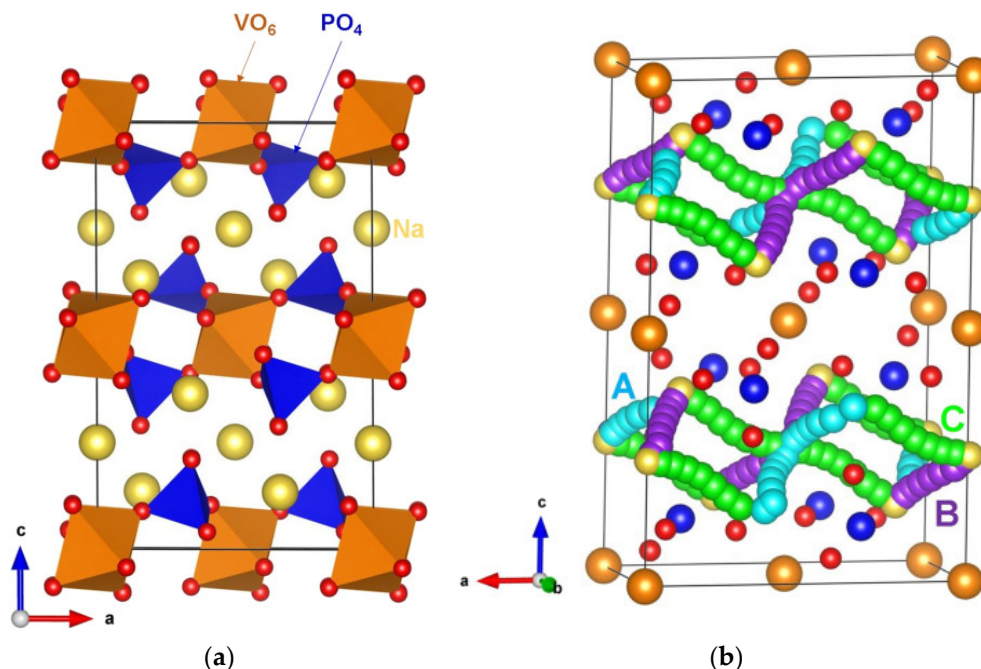


Figure 3. Schematic representation of (a) the crystal structure (space group $C2/c$) and (b) the Na ion diffusion paths along the ab -plane in monoclinic $\text{Na}_3\text{V}(\text{PO}_4)_2$ [94].

3.2. Magnesium-Ion Batteries

Magnesium and calcium are interesting alternative ions to Li, which have the advantage of being divalent [17,45,106–119]. Here we will consider Mg as a potential divalent ion to substitute Li as the diffusion of Ca ions in crystal lattices is plagued by its larger ionic radius. Table 2 reports the activation energies of Mg diffusion in candidate Mg-ion battery materials. It can be observed that there is a very wide range of activation energies (0.52–2.19 eV, refer to Table 2).

Table 2. The activation energies of diffusion of Mg in candidate Mg-ion battery materials.

Material	Activation Energy/eV	Comments
MgV_2O_4	0.52	Ref. [45], 3D
Mg_6MnO_8	0.86	Ref. [109], 3D
MgTiO_3	0.88	Ref. [17]
$\text{Mg}_3\text{Fe}_2\text{Si}_3\text{O}_{12}$	2.19	Ref. [112]

As can be observed in Table 2, MgV_2O_4 is the most promising Mg-ion battery material considered here with an activation energy of Mg-diffusion of 0.52 eV [45]. In more detail, Kuganathan et al. [45] employed atomistic simulations to calculate the energetics and vacancy-mechanism pathway (refer to Figure 4). The Mg local hops cover distances of 3.62 Å (refer to the arrows in Figure 4a) and the activation energy of migration is 0.52 eV (refer to Figure 4b). These local hops can lead to long-range three-dimensional (3D) diffusion. As the diffusion mechanism is 3D there is no preferred plane or direction [45]. In essence, the ionic conductivity in MgV_2O_4 is significant, however, when it is significantly less as compared to Li-diffusion or Na-diffusion [45,47,95].

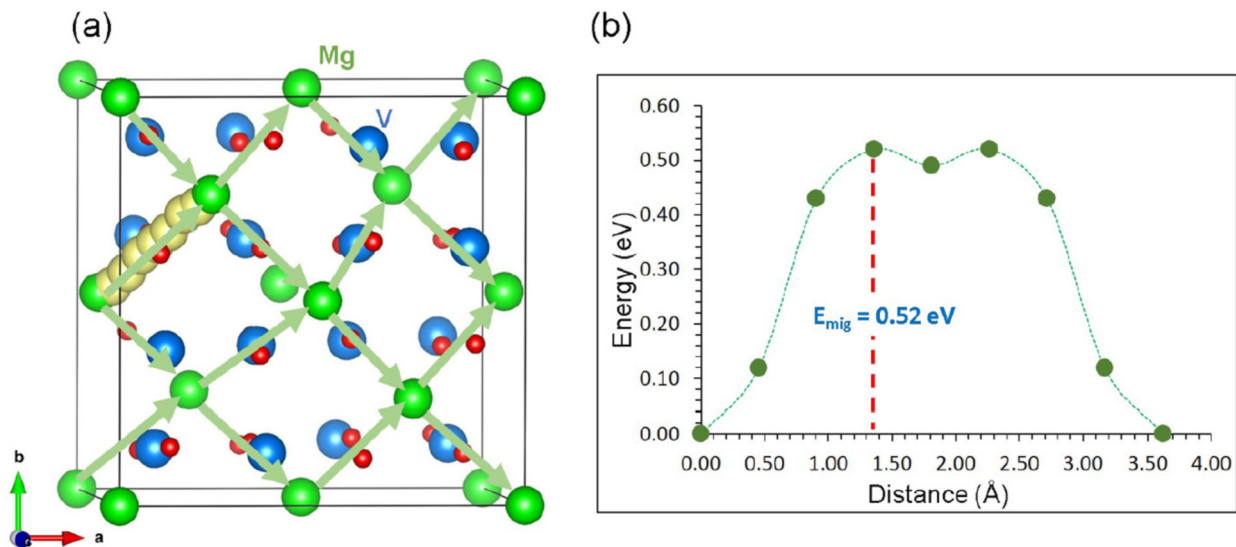


Figure 4. Schematic representation of (a) the Mg ion diffusion paths constructed in MgV_2O_4 and (b) the energy profile diagram for the Mg migration [45].

The computational simulation studies of a range of oxides showed that Mg diffusion is significantly lower as compared to Li (or Na) diffusion, so it is anticipated that these materials in their present form will not be appropriate for energy storage applications.

4. Oxygen Ion Batteries

4.1. Oxygen-Ion Diffusion

Oxygen diffusion is a fundamental property that is very important for oxide materials employed for solid-state ionic materials, fusion materials, etc. Given the applications oxide materials with increased ionic diffusivity have been sought by the community. What is evident is that there is a wide range of oxygen diffusivities depending upon the crystallography, stoichiometry, and composition. Even in similarly structured oxides, for example, in perovskite-related oxides, there is a range of activation energies of oxygen diffusion (refer to Table 3) [120–123]. As can be observed from Table 3 of representative perovskite-related oxides, there is a significant range of activation energies of diffusion [120–123]. Although these oxides have some common structural features (the perovskite block) their differences in composition and stoichiometry lead to differences in activation energies of diffusion of 2.2 eV (refer to Table 3). Additionally, it was established in previous studies (for example [120–123] and references therein) that these materials possess different mechanisms of diffusion in different directions.

Table 3. The activation energies of oxygen diffusion in representative oxides.

Material	Activation Energy/eV	Comments
$\text{La}_2\text{NiO}_{4+\delta}$	0.56	[121], anisotropic mechanism
$\text{GdBaCo}_2\text{O}_{5+\delta}$	0.60	[122]
$\text{Sr}_{0.75}\text{Y}_{0.25}\text{CoO}_{2.625}$	1.56	[123], isotropic mechanism, MD
$\text{La}_{0.8}\text{Sr}_{0.2}\text{MnO}_{3-\delta}$	2.80	[120]

4.2. Oxygen Battery

In the seminal study by Schmid et al. [50] an oxide ion battery was constructed with a $\text{La}_{0.6}\text{Sr}_{0.4}\text{FeO}_{3-\delta}$ (LSF) cathode and a $\text{La}_{0.5}\text{Sr}_{0.5}\text{Cr}_{0.2}\text{Mn}_{0.8}\text{O}_{3-\delta}$ (LSCrMn) anode. Figure 5 shows schematically how the oxygen ion batteries compare with respect to other related electrochemical technologies with respect to their potential power and energy density [50]. The cycling performance was excellent, whereas DC measurements determined capacities up to 120 of A h cm^{-3} at a cell voltage of 0.6 V and a temperature of 350–400 °C [50]. The

study of Schmid et al. [50] showed that mixed ionic electronic conducting-based oxide ion batteries are a possible electrochemical energy storage solution. In a subsequent study, Krammer et al. [124] prepared porous $\text{La}_{0.6}\text{Sr}_{0.4}\text{CoO}_{3-\delta}$ (LSC) thin film electrodes on yttria-stabilized zirconia. They determined that rechargeable oxygen ion batteries efficiently store oxygen by changing the oxygen non-stoichiometry and by the encapsulation of high-pressure oxygen in the closed pores of the cathode [124].

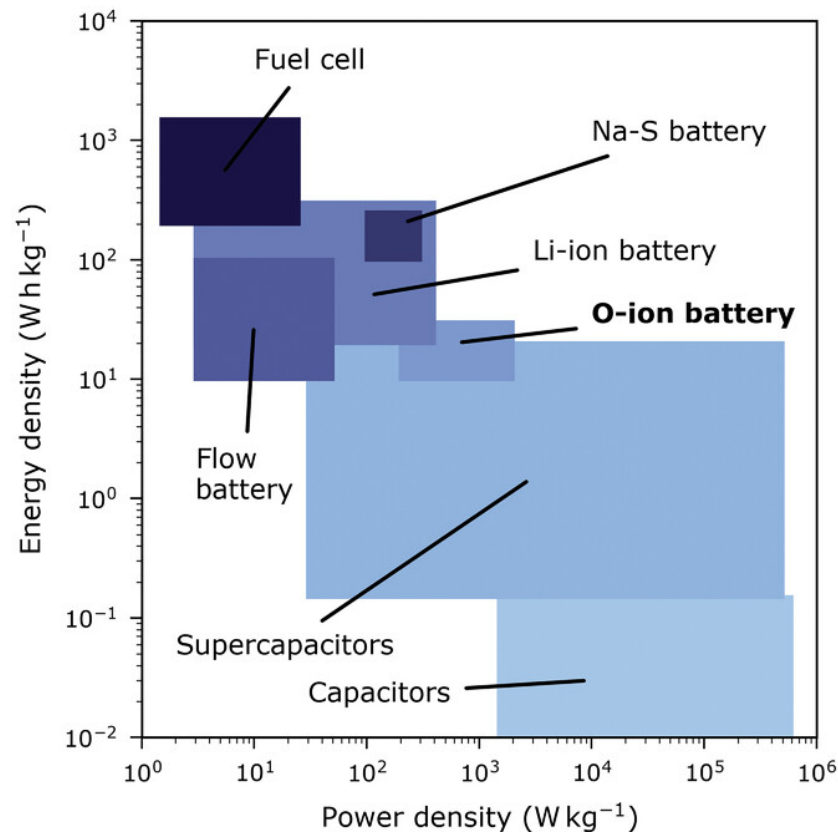


Figure 5. A schematic comparison of the potential power and energy density of oxygen ion batteries with related electrochemical technologies [50].

The high operating temperatures required (typically 200–500 °C) exclude this technology from mobile applications where Li-ion batteries dominate (such as laptops, phones, and cars). Nevertheless, it is a promising technology to store energy where there can be a supply of heat and off-peak electricity production, for example near a civil nuclear reactor. Such an energy storage solution will provide added benefit for the use of centralized nuclear energy production.

5. Tuning the Ionic Diffusion

Tuning the ionic diffusion is typically carried out by doping as discussed above and by forming interfaces or using external parameters such as strain; also, interfaces are important for energy applications [6,7,125–137]. As the energetics of ionic diffusion are governed by the activation energy of diffusion that is in turn the sum of the migration energy of diffusion (i.e., the energy barrier that the ion has to overcome) and the formation energy (i.e., the number of mobile species, so for an oxygen ion migrating via a vacancy mechanism the formation energy of the oxygen vacancy is important) it is necessary for faster diffusion to lower these terms. For example, Kushima and Yildiz [9] employed DFT calculations to predict the optimum strain conditions that would lower the oxygen ion migration energy barriers in strained yttria-stabilized zirconia. Considering the study by Lee et al. [135] it was determined that designed ionic interfaces (heterointerface between

CeO₂ (fluorite) and Y₂O₃ (bixbyite)) can lead to the formation of a very high concentration of interfacial oxygen vacancies. These fluorite-bixbyite interfaces pave the way for the designed formation, transport, and control of oxygen vacancies and may have applications in memristive and ionotronic devices [135]. Notably, the field benefited from the study of Garcia-Barriocanal et al. [6] which determined a colossal enhancement in the ionic conductivity at ZrO₂:Y₂O₃/SrTiO₃ heterostructures. Although there was a lot of research on the claims by Garcia-Barriocanal et al. [6,7,9,127] there was significant focus and progress in the field in the direction of heterointerfaces. As it was seen in Section 3, Mg and Na ions would benefit from an enhancement in the diffusion energetics. What the energy storage community normally investigates first is the impact of the structure and composition (i.e., crystal structure and hypo-hyperstoichiometry) and doping). Future work should also explore the impact of designed heterointerfaces on the diffusion of Mg and Na ions. The key could well be designing the material interfaces rather than exploring exotic crystallographies and compositions. Designed interfaces could offer the concentration of the vehicles required for ionic transport and lower the migration energy barriers.

Doping is an efficient way to tune the migration energy barrier, the number of intrinsic defects required for diffusion, and electronic properties. Considering Na₃Fe₂(PO₄)₃ the lowest energy intrinsic defect process is the Na Frenkel (i.e., the formation of a Na vacancy and Na interstitial pair) [95]. This, in turn, will lead to the formation of Na vacancies that are beneficial for Na ion migration as the vacancy mechanism is energetically favorable [95]. Doping the Fe of the site of Na₃Fe₂(PO₄)₃ with isovalent dopants (M = Sc, La, Gd, and Y) to form Na₃(Fe_xM_{1-x})₂(PO₄)₃ can improve electronic conductivity [95]. Importantly, for Zr doping on the Fe site increases the Na vacancy concentration [95]. Conversely, doping with Si on the P site results in the formation of Na interstitials, which can lead to the enhancement of the capacity of Na₃Fe₂(PO₄)₃. For NaZr₂(PO₄)₃ the Na Frenkel is also the lowest energy intrinsic defect process [47]. Considering isovalent doping it was predicted that K⁺ and Ge⁴⁺ are the significant isovalent dopants on the Na and Zr sites [47]. Doping with Yb, Y, Ga, and In on the Zr site leads to the formation of oxygen vacancies and Na interstitials [47]. Finally, for Na₃V(PO₄)₂ atomistic simulations revealed that the Na-V anti-site defect is the lowest energy intrinsic defect process [94]. Therefore, at high temperatures, there will be some Na ions on the V site and V ions on the Na site [94]. The high energy of the Na Frenkel mechanism will result in very few Na vacancies that are necessary for Na⁺ diffusion. The most efficient strategy to form these Na vacancies is by doping with the tetravalent dopant Ge⁴⁺ on the V site [94]. Notably, Ge doping on the P site increases the Na interstitial concentration that is required for high capacity [94]. Considering MgV₂O₄, Kuganathan et al. [45] showed that doping with cobalt at the vanadium site can lead to the increase of Mg interstitials and O vacancies.

In the fundamental study by Chiabrera et al. [19] it was determined that the control (tuning) of the non-stoichiometry in grain boundaries is an efficient way to enhance the diffusion properties. In particular, Chiabrera et al. [19] showed that the defects induced by strain in the La_{1-x}Sr_xMnO_{3±δ} (LSM) grain boundaries amplify the oxygen diffusion. In essence, with the use of designed interfaces and/or the formation of nanocomposites with appropriate architectures it is possible to tune the material properties of systems for energy applications without the need to use very expensive and scarce materials such as Li or rare-earths.

The kinetics of Na ions (and to a lesser degree Mg) and the continuous and systematic investigation of new novel oxides for energy storage applications are very promising and are expected to compete with Li [138–148]. These ions also have considerable advantages as compared to Li. In particular, Na and Mg are far more abundant, more environmentally friendly, sustainable, and economical as compared to Li. Therefore, should the engineering requirements are met they will make a significant contribution to energy storage from renewable energy and nuclear energy production sites.

6. Summary, Perspective, and Future Outlook

Motivated by explosive lithium demand (for transportation and grid energy storage) and known supply limitations including reserves, regional concentration, mining, and supply chain as well as environmental concerns, the present review considers alternatives to lithium compounds with emphasis on the computational modeling of prospective alternative materials for energy storage. Particular focus is on the defect processes and kinetics of post-lithium oxide batteries. Computational modeling is a tool that can be utilized to provide supplementary information to experiment in order to understand defective oxide materials and optimize them for energy storage applications. Its advantages include aiding experimental work in the characterization of crystal structures, the prediction of the defect diffusion mechanism and energetics, the discovery of the most efficient defect engineering strategies to optimize diffusion, and the fundamental understanding of interfaces and their properties. It is acknowledged that the most interesting systems are usually the ones with the most complicated structures, composition, and stoichiometry. All these constitute their experimental investigation and synthesis difficult. Theoretical calculations can offer a complementary tool to select and focus on the most important systems and there has been also substantial progress in the past years in advanced methodologies. These are now applicable given the ever-increasing computational power and it is anticipated that quantum MD simulations will become a popular tool to investigate the structure, diffusion energetics, and electronic properties of extended systems. Hybrid functionals and meta-GGA approaches are also presently used and these in turn are important when considering the electronic structure of defects. At any rate, deeper analysis will be gained by the traditional methods of analysis such as Brouwer diagrams and the thermodynamic $cB\Omega$ model. These approaches have been embraced, to some extent, by the community in energy-related materials studies. Finally, it is anticipated that advanced techniques based on machine learning will gain ground particularly when a particular material or family of materials will need to be pre-selected for experimental or advanced DFT work. This in turn will accelerate the research and development processes.

A bottleneck for technology is the use of expensive and scarce materials (such as Li, rare-earths, or precious metals) in most advanced technological applications. This is an expensive and unsustainable way that will lead to delay and frustration in the coming years. Many key materials such as rare-earths are mined in China, whereas economic areas such as the EU produce very limited quantities of rare-earths and Li. A future potential reduction in rare-earth or Li exports will have disastrous consequences for numerous industries in many countries. Recycling and/or the discovery of more mines alone will not suffice to provide a sustainable supply of these materials. What is required is to gradually reduce the dependence on scarce materials in advanced technological applications and to move towards cheaper and more available materials. In this respect, the development of energy storage materials based on Na, and to a lesser degree Mg, is the way forward. The development of energy storage systems needs to be assessed considering all steps from cradle to grave. The environmental, economic, and sustainability of storage systems are also important for associated technologies such as renewable energy production and nuclear energy.

Author Contributions: The manuscript was written and edited by all authors. All authors have read and agreed to the published version of the manuscript.

Funding: This research received no external funding.

Institutional Review Board Statement: Not applicable.

Informed Consent Statement: Not applicable.

Conflicts of Interest: The authors declare no conflict of interest.

References

1. Steele, B.C.H. Appraisal of $Ce_{1-y}Gd_yO_{2-y/2}$ electrolytes for IT-SOFC operation at 500 °C. *Solid State Ion.* **2000**, *129*, 95–110. [[CrossRef](#)]
2. Sata, N.; Eberman, K.; Eberl, K.; Maier, J. Mesoscopic fast ion conduction in nanometre scale planar heterostructures. *Nature* **2000**, *408*, 946–949. [[CrossRef](#)] [[PubMed](#)]
3. Singhal, S.C. Advances in solid oxide fuel cell technology. *Solid State Ion.* **2000**, *135*, 305–313. [[CrossRef](#)]
4. Sickafus, K.E.; Minervini, L.; Grimes, R.W.; Valdez, J.A.; Ishimaru, M.; Li, F.; McClellan, K.J.; Hartmann, T. Radiation tolerance of complex oxides. *Science* **2000**, *289*, 748–751. [[CrossRef](#)]
5. Steele, B.C.H.; Heinzl, A. Materials for fuel-cell technologies. *Nature* **2001**, *414*, 345–352. [[CrossRef](#)]
6. Garcia-Barriocanal, J.; Rivera-Calzada, A.; Varela, M.; Sefrioui, Z.; Iborra, E.; Leon, C.; Pennycook, S.J.; Santamaria, J. Colossal ionic conductivity at interfaces of epitaxial $ZrO_2:Y_2O_3/SrTiO_3$ heterostructures. *Science* **2008**, *321*, 676–680. [[CrossRef](#)]
7. Kilner, J.A. Ionic conductors: Feel the strain. *Nat. Mater.* **2008**, *7*, 838. [[CrossRef](#)] [[PubMed](#)]
8. Vovk, R.V.; Obolenskii, M.A.; Zavgorodniy, A.A.; Goulatis, I.L.; Beleskii, V.I.; Chroneos, A. Structural relaxation, metal to insulator transition and pseudo-gap in oxygen deficient $HoBa_2Cu_3O_{7-\delta}$ single crystals. *Phys. C* **2009**, *469*, 203–206. [[CrossRef](#)]
9. Vovk, R.V.; Vovk, N.R.; Shekhovtsov, O.V.; Goulatis, I.L.; Chroneos, A. c-axis hopping conductivity in heavily Pr-doped YBCO single crystals. *Semicond. Sci. Technol.* **2013**, *26*, 085017. [[CrossRef](#)]
10. Rushton, M.J.D.; Chroneos, A.; Skinner, S.J.; Kilner, J.A.; Grimes, R.W. Effect of strain on the oxygen diffusion in yttria and gadolinia co-doped ceria. *Solid State Ion.* **2013**, *230*, 37–42. [[CrossRef](#)]
11. Rushton, M.J.D.; Chroneos, A. Impact of uniaxial strain and doping on oxygen diffusion in CeO_2 . *Sci. Rep.* **2014**, *4*, 6068. [[CrossRef](#)]
12. Lumley, S.C.; Grimes, R.W.; Murphy, S.T.; Burr, P.A.; Chroneos, A.; Chard-Tuckey, P.R.; Wenman, M.R. The thermodynamics of hydride precipitation: The importance of entropy, enthalpy and disorder. *Acta Mater.* **2014**, *79*, 351–362. [[CrossRef](#)]
13. Tomkiewicz, A.C.; Tamimi, A.; Huq, A.; McIntosh, S. Oxygen transport pathways in Ruddlesden–Popper structured oxides revealed via in situ neutron diffraction. *J. Mater. Chem. A* **2015**, *3*, 21864–21874. [[CrossRef](#)]
14. Ning, D.; Baki, A.; Scherb, T.; Song, J.; Fantin, A.; Liu, X.Z.; Schumacher, G.; Banhart, J.; Bouwmeester, H.J.M. Influence of A-site deficiency on structural evolution of $Pr_{2-x}NiO_{4+\delta}$ with temperature. *Solid State Ion.* **2019**, *342*, 115056. [[CrossRef](#)]
15. Solovjov, A.L.; Petrenko, E.V.; Omelchenko, L.V.; Vovk, R.V.; Goulatis, I.L.; Chroneos, A. Effect of annealing on a pseudogap state in untwinned $YBa_2Cu_3O_{7-\delta}$ single crystals. *Sci. Rep.* **2019**, *9*, 9274. [[CrossRef](#)] [[PubMed](#)]
16. Kuganathan, N.; Iyngaran, P.; Vovk, R.; Chroneos, A. Defects, dopants and Mg diffusion in $MgTiO_3$. *Sci. Rep.* **2019**, *9*, 4394. [[CrossRef](#)]
17. Chiabrera, F.; Garbayo, I.; Lopez-Conesa, L.; Martin, G.; Ruiz-Caridad, A.; Walls, M.; Ruiz-Gonzalez, L.; Kordatos, A.; Nunez, M.; Morata, A.; et al. Engineering transport in manganites by tuning local nonstoichiometry in grain boundaries. *Adv. Mater.* **2019**, *31*, 1805360. [[CrossRef](#)]
18. Acosta, M.; Baiutti, F.; Tarancon, A.; MacManus-Driscoll, J.L. Nanostructured materials and interfaces for advanced ionic electronic conducting oxides. *Adv. Mater. Interfaces* **2019**, *6*, 1–15. [[CrossRef](#)]
19. Zou, Z.; Ma, N.; Wang, A.; Ran, Y.; Song, T.; Jiao, Y.; Liu, J.; Zhou, H.; Shi, W.; He, B.; et al. Relationships between Na^+ distribution, concerted migration, and diffusion properties in rhombohedral NASICON. *Adv. Energy Mater.* **2020**, *10*, 2001486. [[CrossRef](#)]
20. Shi, J.; Han, C.; Niu, H.; Zhu, Y.; Yun, S. Theoretical investigation of proton diffusion in Dion-Jacobson layered perovskite $RbBiNb_2O_7$. *Nanomaterials* **2021**, *11*, 1953. [[CrossRef](#)]
21. Wang, F.; Xing, Y.; Hu, E.; Wang, J.; Shi, J.; Yun, S.; Zhu, B. PN heterostructure interface-facilitated proton conduction in 3C-SiC/ $Na_{0.6}CoO_2$ electrolyte for fuel cell application. *ACS Appl. Energy Mater.* **2021**, *4*, 7519–7525. [[CrossRef](#)]
22. Grieshammer, S.; Belova, I.V.; Murch, G.E. Thermodiffusion and ion transport in doped ceria by molecular dynamics simulations. *Acta Mater.* **2021**, *210*, 116802. [[CrossRef](#)]
23. Varley, J.B.; Shen, B.; Higashiwaki, M. Wide bandgap semiconductor materials and devices. *J. Appl. Phys.* **2022**, *131*, 230401. [[CrossRef](#)]
24. Hassan, J.Z.; Raza, A.; Qumar, U.; Li, G. Recent advances in engineering strategies of Bi-based photocatalysts for environmental remediation. *Sust. Mater. Technol.* **2022**, *33*, e00478. [[CrossRef](#)]
25. Yattoo, M.A.; Seymour, I.D.; Skinner, S.J. Neutron diffraction and DFT studies of oxygen defect and transport in higher-order Ruddlesden–Popper phase materials. *RSC Adv.* **2023**, *13*, 13786–13797. [[CrossRef](#)]
26. Feng, Z.; Yang, J.; NuLi, Y.; Wang, J. Sol–gel synthesis of $Mg_{1.03}Mn_{0.97}SiO_4$ and its electrochemical intercalation behavior. *J. Power Sources* **2008**, *184*, 604–609. [[CrossRef](#)]
27. Schichtel, N.; Korte, C.; Hesse, D.; Janek, J. Elastic strain at interfaces and its influence on ionic conductivity in nanoscaled solid electrolyte thin films- theoretical considerations and experimental studies. *Phys. Chem. Chem. Phys.* **2009**, *11*, 3043–3048. [[CrossRef](#)]
28. Vovk, R.V.; Nazyrov, Z.F.; Obolenskii, M.A.; Goulatis, I.L.; Chroneos, A.; Simoes, V.M.P. Phase separation in oxygen deficient $HoBa_2Cu_3O_{7-\delta}$ single crystals: Effect of pressure and twin boundaries. *Phil. Mag.* **2011**, *91*, 2291–2302. [[CrossRef](#)]
29. Serras, P.; Palomares, V.; Goñi, A.; Gil de Muro, I.; Kubiak, P.; Lezama, L.; Rojo, T. High voltage cathode materials for Na-ion batteries of general formula $Na_3V_2O_{2x}(PO_4)_2F_{3-2x}$. *J. Mater. Chem.* **2012**, *22*, 22301–22308. [[CrossRef](#)]

30. Tripathi, R.; Wood, S.M.; Islam, M.S.; Nazar, L.F. Na-ion mobility in layered $\text{Na}_2\text{FePO}_4\text{F}$ and olivine $\text{Na}[\text{Fe},\text{Mn}]\text{PO}_4$. *Energy Environ. Sci.* **2013**, *6*, 2257–2264. [[CrossRef](#)]
31. Clark, J.M.; Barpanda, P.; Yamada, A.; Islam, M.S. Sodium-ion battery cathodes $\text{Na}_2\text{FeP}_2\text{O}_7$ and $\text{Na}_2\text{MnP}_2\text{O}_7$: Diffusion behavior for high rate performance. *J. Mater. Chem. A* **2014**, *2*, 11807–11812. [[CrossRef](#)]
32. Orikasa, Y.; Masese, T.; Koyama, Y.; Mori, T.; Hattori, M.; Yamamoto, K.; Okado, T.; Huang, Z.D.; Minato, T.; Tassel, C.; et al. High energy density rechargeable magnesium battery using earth-abundant and non-toxic elements. *Sci. Rep.* **2014**, *4*, 5622. [[CrossRef](#)] [[PubMed](#)]
33. Lee, S.H.; DiLeo, R.A.; Marschlok, A.C.; Takeuchi, K.J.; Takeuchi, E.S. Sol gel based synthesis and electrochemistry of magnesium vanadium oxide: A promising cathode material for secondary magnesium ion batteries. *ECS Electrochem. Lett.* **2014**, *3*, A87. [[CrossRef](#)]
34. Huang, Z.D.; Masese, T.; Orikasa, Y.; Mori, T.; Minato, T.; Tassel, C.; Kobayashi, Y.; Kageyama, H.; Uchimoto, Y. MgFePO_4F as a feasible cathode material for magnesium batteries. *J. Mater. Chem. A* **2014**, *2*, 11578. [[CrossRef](#)]
35. Jay, E.E.; Rushton, M.J.D.; Chroneos, A.; Grimes, R.W.; Kilner, J.A. Genetics of superionic conductivity in lithium lanthanum titanates. *Phys. Chem. Chem. Phys.* **2015**, *17*, 178–183. [[CrossRef](#)] [[PubMed](#)]
36. Yun, S.; Zhou, X.; Even, J.; Hagfeldt, A. Theoretical treatment of $\text{CH}_3\text{NH}_3\text{PbI}_3$ perovskite solar cells. *Angew. Chem.* **2017**, *56*, 15806–15817. [[CrossRef](#)]
37. Zhu, J.; Vasilopoulou, M.; Davazoglou, D.; Kennou, S.; Chroneos, A.; Schwingenschlögl, U. Intrinsic defects and H doping in WO_3 . *Sci. Rep.* **2017**, *7*, 40882. [[CrossRef](#)]
38. Kim, J.; Yoon, G.; Kim, H.; Park, Y.U.; Kang, K. $\text{Na}_3\text{V}(\text{PO}_4)_2$: A new layered-type cathode material with high water stability and power capability for Na-ion batteries. *Chem. Mater.* **2018**, *30*, 3683–3689. [[CrossRef](#)]
39. Kuganathan, N.; Kordatos, A.; Fitzpatrick, M.E.; Vovk, R.V.; Chroneos, A. Defect process and lithium diffusion in Li_2TiO_3 . *Solid State Ion.* **2018**, *327*, 93–98. [[CrossRef](#)]
40. Kuganathan, N.; Kordatos, A.; Chroneos, A. Li_2SnO_3 as a cathode material for lithium-ion batteries: Defects, lithium ion diffusion and dopants. *Sci. Rep.* **2018**, *8*, 12621. [[CrossRef](#)]
41. Kuganathan, N.; Chroneos, A. Defects, dopants and sodium mobility in $\text{Na}_2\text{MnSiO}_4$. *Sci. Rep.* **2018**, *8*, 14669. [[CrossRef](#)] [[PubMed](#)]
42. Kuganathan, N.; Chroneos, A. Defects and dopant properties of $\text{Li}_3\text{V}_2(\text{PO}_4)_3$. *Sci. Rep.* **2019**, *9*, 333.
43. Liu, T.; Zhang, Y.; Jiang, Z.; Zeng, X.; Ji, J.; Li, Z.; Gao, X.; Sun, M.; Lin, Z.; Ling, M.; et al. Exploring competitive features of stationary sodium ion batteries for electrochemical energy storage. *Energy Environ. Sci.* **2019**, *12*, 1512–1533. [[CrossRef](#)]
44. Tsuruoka, T.; Tsujita, T.; Su, J.; Nishitani, Y.; Hamamura, T.; Inatomi, Y.; Nakura, K.; Terabe, K. Fabrication of a magnesium-ion conducting magnesium phosphate electrolyte film using atomic layer deposition. *Jpn. J. Appl. Phys.* **2020**, *59*, SIIG08. [[CrossRef](#)]
45. Kuganathan, N.; Davazoglou, K.; Chroneos, A. Computer modelling investigation of MgV_2O_4 for Mg-ion batteries. *J. Appl. Phys.* **2020**, *127*, 035106. [[CrossRef](#)]
46. Kuganathan, N.; Rushton, M.J.D.; Grimes, R.W.; Kilner, J.A.; Gkanas, E.I.; Chroneos, A. Self-diffusion in garnet-type $\text{Li}_7\text{La}_3\text{Zr}_2\text{O}_{12}$ solid electrolytes. *Sci. Rep.* **2021**, *11*, 451. [[CrossRef](#)]
47. Kuganathan, N.; Chroneos, A. Defects, diffusion, dopants and encapsulation of Na in $\text{NaZr}_2(\text{PO}_4)_3$. *Materialia* **2021**, *16*, 101039. [[CrossRef](#)]
48. Hasa, I.; Mariyappan, S.; Saurel, D.; Adelmhelm, P.; Kuposov, A.Y.; Masquelier, C.; Croguennec, L.; Casas-Cabanas, M. Challenges of today for Na-based batteries of the future: From materials to cell metrics. *J. Power Sources* **2021**, *482*, 228872. [[CrossRef](#)]
49. Rex, K.A.; Iyngaran, P.; Kuganathan, N.; Chroneos, A. Defect properties and lithium incorporation in Li_2ZrO_3 . *Energies* **2021**, *14*, 3963. [[CrossRef](#)]
50. Schmid, A.; Krammer, M.; Fleig, J. Rechargeable oxide ion batteries based on mixed conducting oxide electrodes. *Adv. Energy Mater.* **2023**, *13*, 2203789. [[CrossRef](#)]
51. Smith, W.; Forester, T.R. DL_POLY_2.0: A general-purpose parallel molecular dynamics simulation package. *J. Mol. Graph.* **1996**, *14*, 136. [[CrossRef](#)] [[PubMed](#)]
52. Gale, J.D. GULP: A computer program for the symmetry-adapted simulation of solids. *J. Chem. Soc. Faraday Trans.* **1997**, *93*, 629. [[CrossRef](#)]
53. Catlow, C.R.A. (Ed.) *Computer Modelling in Inorganic Crystallography*, 1st ed.; Academic Press: San Diego, CA, USA, 1997.
54. Segall, M.D.; Lindan, P.J.D.; Probert, M.J.; Pickard, C.J.; Hasnip, P.J.; Clark, S.J.; Payne, M.C. First-principles simulation: Ideas, illustrations and the CASTEP code. *J. Phys. Condens. Matter* **2002**, *14*, 2717. [[CrossRef](#)]
55. Hohenberg, P.; Kohn, W. Inhomogeneous electron gas. *Phys. Rev.* **1964**, *136*, B864. [[CrossRef](#)]
56. Kohn, W. Nobel Lecture: Electronic structure of matter—Wave functions and density functionals. *Rev. Mod. Phys.* **1998**, *71*, 1253. [[CrossRef](#)]
57. Koch, W.; Holthausen, M.C. *A Chemist's Guide to Density Functional Theory*; Wiley-VCH: Weinheim, Germany, 2001.
58. Henkelman, G.; Uberuaga, B.P.; Jónsson, H. A climbing image nudged elastic band method for finding saddle points and minimum energy paths. *J. Chem. Phys.* **2000**, *113*, 9901. [[CrossRef](#)]
59. Born, M.; Mayer, J.E. Zur Gittertheorie der Ionenkristalle. *Z. Phys.* **1932**, *75*, 1. [[CrossRef](#)]
60. Buckingham, R.A. The classical equation of state of gaseous helium, neon and argon. *Proc. R. Soc. Lond. Ser. A* **1938**, *168*, 264.

61. Grimes, R.W.; Busker, G.; McCoy, M.A.; Chroneos, A.; Kilner, J.A.; Chen, S.P. The effect of ion size on solution mechanism and defect cluster geometry. *Ber. Bunsenges. Phys. Chem.* **1997**, *101*, 1204. [[CrossRef](#)]
62. Busker, G.; Chroneos, A.; Grimes, R.W.; Chen, I.W. Solution Mechanisms for Dopant Oxides in Yttria. *J. Am. Ceram. Soc.* **1999**, *82*, 1553. [[CrossRef](#)]
63. Varotsos, P. Calculation of the migration volume of vacancies in ionic solids from macroscopic parameters. *Phys. Stat. Sol.* **1978**, *47*, K133–K136. [[CrossRef](#)]
64. Varotsos, P. Comparison of models that interconnect point defect parameters in solids with bulk properties. *J. Appl. Phys.* **2007**, *101*, 123503. [[CrossRef](#)]
65. Varotsos, P. Point defect parameters in β -PbF₂ revisited. *Solid State Ion.* **2008**, *179*, 438–441. [[CrossRef](#)]
66. Zhang, B.; Wu, X.; Xu, J.; Zhou, R. Application of the $cB\Omega$ model for the calculation of oxygen self-diffusion coefficients in minerals. *J. Appl. Phys.* **2010**, *108*, 053505. [[CrossRef](#)]
67. Vallianatos, F.; Saltas, V. Application of the $cB\Omega$ model to the calculation of diffusion parameters of He in olivine. *Phys. Chem. Miner.* **2014**, *41*, 181–188. [[CrossRef](#)]
68. Cooper, M.W.D.; Grimes, R.W.; Fitzpatrick, M.E.; Chroneos, A. Modeling oxygen self-diffusion in UO₂ under pressure. *Solid State Ion.* **2015**, *282*, 26–30. [[CrossRef](#)]
69. Zhang, B.; Shan, S. Application of the $cB\Omega$ model to the calculation of diffusion parameters of Si in silicates. *Geochem. Geophys. Geosyst.* **2015**, *16*, 705–718. [[CrossRef](#)]
70. Chroneos, A.; Vovk, R.V. Modeling self-diffusion in UO₂ and ThO₂ by connecting point defect parameters with bulk properties. *Solid State Ion.* **2015**, *274*, 1–3. [[CrossRef](#)]
71. Parfitt, D.C.; Cooper, M.W.D.; Rushton, M.J.D.; Christopoulos, S.-R.G.; Fitzpatrick, M.E.; Chroneos, A. Thermodynamic calculations of oxygen self-diffusion in mixed-oxide nuclear fuels. *RSC Adv.* **2016**, *6*, 74018–74028. [[CrossRef](#)]
72. Saltas, V.; Chroneos, A.; Vallianatos, F.A. A thermodynamic approach of self- and hetero-diffusion in GaAs: Connecting point defect parameters with bulk properties. *RSC Adv.* **2016**, *6*, 53324–53330. [[CrossRef](#)]
73. Chroneos, A. Connecting point defect parameters with bulk properties to describe diffusion in solids. *Appl. Phys. Rev.* **2016**, *3*, 041304. [[CrossRef](#)]
74. Sarlis, N.V.; Skordas, E.S. Estimating the compressibility of osmium from recent measurements of Ir-Os alloys under high pressure. *J. Phys. Chem. A* **2016**, *120*, 1601–1604. [[CrossRef](#)] [[PubMed](#)]
75. Skordas, E.S.; Sarlis, N.V.; Varotsos, P.A. Applying the $cB\Omega$ thermodynamical model to LiF using its equation of state obtained from high pressure diamond anvil cell measurements. *Solid State Ion.* **2020**, *354*, 115404. [[CrossRef](#)]
76. Sanchez, J.M.; Ducastelle, F.; Gratias, D. Generalized cluster description of multicomponent systems. *Phys. A* **1984**, *128*, 334–350. [[CrossRef](#)]
77. Wei, S.H.; Ferreira, L.G.; Bernard, J.E.; Zunger, A. Electronic properties of random alloys: Special quasirandom structures. *Phys. Rev. B* **1990**, *42*, 9622–9649. [[CrossRef](#)]
78. Zunger, A.; Wei, S.H.; Ferreira, L.G.; Bernard, J.E. Special quasirandom structures. *Phys. Rev. Lett.* **1990**, *65*, 353–356. [[CrossRef](#)]
79. Laks, D.B.; Ferreira, L.G.; Froyen, S.; Zunger, A. Efficient cluster expansion for substitutional systems. *Phys. Rev. B* **1992**, *46*, 12587–12605. [[CrossRef](#)]
80. Wolverton, C.; Zunger, A. Ising-like description of structurally released ordered and disordered alloys. *Phys. Rev. Lett.* **1995**, *75*, 3162–3165. [[CrossRef](#)]
81. Jiang, C.; Sordelet, D.J.; Gleeson, B. First-principles study of phase stability in pseudobinary (Ni_{1-x}Pt_x)₃Al. *Phys. Rev. B* **2005**, *72*, 184203. [[CrossRef](#)]
82. Chroneos, A.; Jiang, C.; Grimes, R.W.; Schwingenschlögl, U.; Bracht, H. Defect interactions in Sn_{1-x}Ge_x alloys. *Appl. Phys. Lett.* **2009**, *94*, 252104. [[CrossRef](#)]
83. Chroneos, A.; Jiang, C.; Grimes, R.W.; Schwingenschlögl, U.; Bracht, H. E centers in Si_{1-x-y}Ge_xSn_y alloys. *Appl. Phys. Lett.* **2009**, *95*, 112101. [[CrossRef](#)]
84. Murphy, S.T.; Chroneos, A.; Jiang, C.; Schwingenschlögl, U.; Grimes, R.W. Deviations from Vegard's law in ternary III-V alloys. *Phys. Rev. B* **2010**, *82*, 073201. [[CrossRef](#)]
85. Murphy, S.T.; Chroneos, A.; Grimes, R.W.; Jiang, C.; Schwingenschlögl, U. Phase stability and the arsenic vacancy defect in In_xGa_{1-x}As. *Phys. Rev. B* **2011**, *84*, 184108. [[CrossRef](#)]
86. Wang, H.; Chroneos, A.; Jiang, C.; Schwingenschlögl, U. Modelling zirconium hydrides using the special quasirandom structure approach. *Phys. Chem. Chem. Phys.* **2013**, *15*, 7599–7603. [[CrossRef](#)]
87. Chroneos, A.; Rushton, M.J.D.; Jiang, C.; Tsoukalas, L.H. Nuclear wasteform materials: Atomistic simulation case studies. *J. Nucl. Mater.* **2013**, *441*, 29–39. [[CrossRef](#)]
88. Jiang, C.; Chroneos, A. Ab initio modelling of MAX phase solid solutions using the special quasirandom structure approach. *Phys. Chem. Chem. Phys.* **2018**, *20*, 1173–1180. [[CrossRef](#)] [[PubMed](#)]
89. Chen, C.Y.; Matsumoto, K.; Nohira, T.; Hagiwara, R. Na₂MnSiO₄ as a positive electrode material for sodium secondary batteries using an ionic liquid electrolyte. *Electrochem. Commun.* **2014**, *45*, 63–66. [[CrossRef](#)]
90. Kosova, N.V.; Podugolnikov, V.R.; Devyatkina, E.T.; Slobodyuk, A.B. Structure and electrochemistry of NaFePO₄ and Na₂FePO₄F cathode materials prepared via mechanochemical route. *Mater. Res. Bull.* **2014**, *60*, 849–857. [[CrossRef](#)]

91. Han, M.H.; Gonzalo, E.; Singh, G.; Rojo, T. A comprehensive review of sodium layered oxides: Powerful cathodes for Na-ion batteries. *Energy Environ. Sci.* **2015**, *8*, 81–102. [[CrossRef](#)]
92. Fang, Y.; Liu, Q.; Xiao, L.; Ai, X.; Yang, H.; Cao, Y. High-Performance Olivine NaFePO₄ Microsphere Cathode Synthesized by Aqueous Electrochemical Displacement Method for Sodium Ion Batteries. *ACS Appl. Mater. Interfaces* **2015**, *7*, 17977–17984. [[CrossRef](#)]
93. Hang, X.; Rui, X.; Chen, D.; Tan, H.; Yang, D.; Huang, S.; Yu, Y. Na₃V₂(PO₄)₃: An advanced cathode for sodium-ion batteries. *Nanoscale* **2019**, *11*, 2556–2576.
94. Kuganathan, N.; Chroneos, A. Na₃V(PO₄)₂ cathode material for Na ion batteries: Defect, dopants and Na diffusion. *Solid State Ion.* **2019**, *336*, 75–79. [[CrossRef](#)]
95. Kuganathan, N.; Chroneos, A. Defect chemistry and Na-ion diffusion in Na₃Fe₂(PO₄)₃. *Materials* **2019**, *12*, 1348. [[CrossRef](#)]
96. Kaushalya, R.; Iyngaran, P.; Kuganathan, N.; Chroneos, A. Defect, diffusion and dopant properties of NaNiO₂: Atomistic simulation study. *Energies* **2019**, *12*, 3094. [[CrossRef](#)]
97. Kuganathan, N.; Kelaidis, N.; Chroneos, A. Defect chemistry, sodium diffusion and doping behaviour in NaFeO₂. *Materials* **2019**, *12*, 3243. [[CrossRef](#)]
98. Pak, Y.C.; Rim, C.H.; Hwang, S.G.; Ri, K.C.; Yu, C.J. Defect formation and ambivalent effects on electrochemical performance in layered sodium titanate Na₂Ti₃O₇. *Phys. Chem. Chem. Phys.* **2023**, *25*, 3420–3431. [[CrossRef](#)] [[PubMed](#)]
99. Apostolova, I.N.; Apostolov, A.T.; Wesselinowa, J.M. Band gap energy of ion-doped multiferroic NaFeO₂ nanoparticles. *Phys. Status Solidi RRL* **2023**, 2300159. [[CrossRef](#)]
100. Wu, H.L.; Chen, Y.Q.; Wen, T.Z.; Chen, L.; Pu, X.J.; Chen, Z.X. Advances in vanadium-redoxed polyanions for high-voltage sodium-ion batteries. *Batteries* **2023**, *9*, 56. [[CrossRef](#)]
101. Paidi, A.K.; Sharma, A.; Paidi, V.K.; Illa, M.P.; Lee, K.S.; Lee, S.S.; Ahn, D.; Mukhopadhyay, A. Na₂ZrFe(PO₄)₃- A Rhombohedral NASICON-Structured Material: Synthesis, Structure and Na-Intercalation Behavior. *Inorg. Chem.* **2023**, *62*, 4124–4135. [[CrossRef](#)]
102. Ji, Y.Z.; Honma, T.; Komatsu, T. Formation of sodium ion conductive NaZr₂(PO₄)₃ composite via liquid phase sintering method with sodium disilicate glass. *Solid State Ion.* **2023**, *395*, 116213. [[CrossRef](#)]
103. Satrughna, J.A.K.; Kanwade, A.; Srivastava, A.; Tiwara, M.K.; Yadav, S.C.; Akula, S.T.; Shirage, P.M. Experimental and ab initio based DFT calculation of NaFe_{0.5}Co_{0.5}O₂ as an excellent cathode material for futuristic sodium ion batteries. *J. Energy Storage* **2023**, *65*, 107371. [[CrossRef](#)]
104. Gomez-Garduno, N.; Araiza, D.G.; Celaya, C.A.; Muniz, J.; Pfeiffer, H. Unveiling the different physicochemical properties of M-doped beta-NaFeO₂ (where M = Ni or Cu) materials evaluated as CO₂ sorbents: A combined experimental and theoretical analysis. *J. Mater. Chem. A* **2023**, *11*, 10938–10954. [[CrossRef](#)]
105. Zhang, X.T.; Tian, H.L.; Zhang, Y.H.; Cai, Y.J.; Yao, X.; Su, Z. Diatomic-doped carbon layer decorated Na₃V₂(PO₄)₂F₃ as a durable ultrahigh-stability cathode for sodium ion batteries. *New J. Chem.* **2023**, *47*, 9611–9617. [[CrossRef](#)]
106. Aurbach, D.; Gofer, Y.; Lu, Z.; Schechter, A.; Chusid, O.; Gizbar, H.; Cohen, Y.; Ashkenazi, V.; Moshkovich, M.; Turgeman, R.; et al. A short review on the comparison between Li battery systems and rechargeable magnesium battery technology. *J. Power Sources* **2001**, *97–98*, 28–32. [[CrossRef](#)]
107. Muldoon, J.; Bucur, C.B.; Gregory, T. Quest for Nonaqueous Multivalent Secondary Batteries: Magnesium and Beyond. *Chem. Rev.* **2014**, *114*, 11683–11720. [[CrossRef](#)] [[PubMed](#)]
108. Pnrouch, A.; Frontera, C.; Bardé, F.; Palacín, M.R. Towards a calcium-based rechargeable battery. *Nat. Mater.* **2015**, *15*, 169–172. [[CrossRef](#)]
109. Gummow, R.J.; Vamvounis, G.; Kannan, M.B.; He, Y. Calcium-Ion Batteries: Current State-of-the-Art and Future Perspectives. *Adv. Mater.* **2018**, *30*, 1801702. [[CrossRef](#)]
110. Kuganathan, N.; Gkanas, E.I.; Chroneos, A. Mg₆MnO₈ as a magnesium-ion battery material: Defects, dopants and Mg-ion transport. *Energies* **2019**, *12*, 3213. [[CrossRef](#)]
111. Kuganathan, N.; Ganeshalingam, S.; Chroneos, A. Defect, transport, and dopant properties of andradite garnet Ca₃Fe₂Si₃O₁₂. *AIP Adv.* **2020**, *10*, 075004. [[CrossRef](#)]
112. Kuganathan, N.; Chroneos, A. Defect and dopants in CaFeSi₂O₆: Classical and DFT simulations. *Energies* **2020**, *13*, 1285. [[CrossRef](#)]
113. Kuganathan, N.; Chroneos, A. Atomic-scale studies of garnet-type Mg₃Fe₂Si₃O₁₂: Defect chemistry, diffusion and dopant properties. *J. Power Sources Adv.* **2020**, *3*, 100016. [[CrossRef](#)]
114. Kuganathan, N.; Chroneos, A. Defect and dopant properties in CaMnO₃. *AIP Adv.* **2021**, *11*, 055106. [[CrossRef](#)]
115. Torres, A.; Casals, J.L.; Arroyo de Dompablo, M.E. Enlisting potential cathode materials for rechargeable Ca batteries. *Chem. Mater.* **2021**, *33*, 2488–2497. [[CrossRef](#)]
116. Tekliye, D.B.; Kumar, A.; Weihang, X.; Mercy, T.D.; Canepa, P.; Gautam, G.S. Exploration of NASICON frameworks as calcium-ion battery electrodes. *Chem. Mater.* **2022**, *34*, 10133–10143. [[CrossRef](#)]
117. Liu, D.W.; Chen, X.H.; Zhang, Q.J.; Li, J.C.; Yan, F.F.; Dai, H.Y.; Wang, X.Z.; Chen, J.; Zhai, X.Z. Effects of Mg-doping on distorted structure and enhanced electrochemical performance of V_{1-x}Mg_xO₂ nanorods. *Mater. Today Energy* **2022**, *33*, 104948.
118. Zhang, X.; Li, D.; Ruan, Q.; Liu, L.; Wang, B.; Xiong, F.; Huang, C.; Chu, P. Vanadium-based cathode materials for rechargeable magnesium batteries. *Mater. Today Energy* **2023**, *32*, 101232. [[CrossRef](#)]

119. Lagunas, F.; Alexander, G.; Punaro, A.L.; Moscosa, C.; Hu, L.H.; Cabana, J.; Klie, R.F. Structural transformations at the atomic scale in spinel vanadium oxides upon Mg^{2+} extraction. *ACS Appl. Energy Mater.* **2023**, *6*, 5681–5689. [[CrossRef](#)]
120. Mauvy, F.; Bassat, J.M.; Boehm, E.; Dordor, P.; Grenier, J.C.; Loup, J.P. Chemical oxygen diffusion coefficient measurement by conductivity relaxation—Correlation between tracer diffusion coefficient and chemical diffusion coefficient. *J. Eur. Ceram. Soc.* **2004**, *24*, 1265–1269. [[CrossRef](#)]
121. Boehm, E.; Bassat, J.M.; Dordor, P.; Mauvy, F.; Grenier, J.C.; Stevens, P. Oxygen diffusion and transport properties in non-stoichiometric $Ln_{2-x}NiO_{4+\delta}$ oxides. *Solid State Ion.* **2005**, *176*, 2717–2725. [[CrossRef](#)]
122. Tarancon, A.; Marrero-Lopez, D.; Pena-Martinez, J.; Ruiz-Morales, J.C.; Nunez, P. Effect of phase transition on high-temperature electrical properties of $GdBaCo_2O_{5+x}$ layered perovskite. *Solid State Ion.* **2008**, *179*, 611–618. [[CrossRef](#)]
123. Rupasov, D.; Chroneos, A.; Parfitt, D.; Kilner, J.A.; Grimes, R.W.; Istomin, S.Y.; Antipov, E.V. Oxygen diffusion in $Sr_{0.75}Y_{0.25}CoO_{2.625}$: A molecular dynamics study. *Phys. Rev.* **2009**, *79*, 172102. [[CrossRef](#)]
124. Krammer, M.; Schmid, A.; Kubicek, M.; Feig, J. Utilizing oxygen gas storage in rechargeable oxygen ion batteries. *J. Power Sources* **2023**, *577*, 233167. [[CrossRef](#)]
125. Korte, C.; Schichtel, N.; Hesse, D.; Janek, J. Influence of interface structure on mass transport in phase boundaries between different ionic materials: Experimental studies and formal considerations. *Monatsh. Chem.* **2009**, *140*, 1069–1080. [[CrossRef](#)]
126. Cavallaro, A.; Burriel, M.; Roqueta, J.; Apostolidis, A.; Bernardi, A.; Tarancón, A.; Srinivasan, R.; Cook, S.N.; Fraser, H.L.; Kilner, J.A.; et al. Electronic nature of the enhanced conductivity in YSZ-STO multilayers deposited by PLD. *Solid State Ion.* **2010**, *181*, 592–601. [[CrossRef](#)]
127. Pennycook, T.J.; Beck, M.J.; Varga, K.; Varela, M.; Pennycook, S.J.; Pantelides, S.T. Origin of colossal ionic conductivity in oxide multilayers: Interface induced sublattice disorder. *Phys. Rev. Lett.* **2010**, *104*, 115901. [[CrossRef](#)]
128. De Souza, R.A.; Ramadan, A.; Hörner, S. Modifying the barriers for oxygen-vacancy migration in fluorite-structured CeO_2 electrolytes through strain; A computer simulation study. *Energy Environ. Sci.* **2012**, *5*, 5445–5453. [[CrossRef](#)]
129. Navickas, E.; Huber, T.M.; Chen, Y.; Hetaba, W.; Holzlechner, G.; Rupp, G.; Stöger-Pollach, M.; Friedbacher, G.; Hutter, H.; Yildiz, B.; et al. Fast oxygen exchange and diffusion kinetics of grain boundaries in Sr-doped $LaMnO_3$ thin films. *Phys. Chem. Chem. Phys.* **2015**, *17*, 7659–7669. [[CrossRef](#)]
130. Saranya, A.M.; Pla, D.; Morata, A.; Cavallaro, A.; Canales-Vazquez, J.; Kilner, J.A.; Burriel, M.; Tarancon, A. Engineering mixed ionic electronic conduction in $La_{0.8}Sr_{0.2}MnO_{3+\delta}$ nanostructures through fast grain boundary oxygen diffusivity. *Adv. Energy Mater.* **2015**, *5*, 1500377. [[CrossRef](#)]
131. Sun, L.; Marrocchelli, D.; Yildiz, B. Edge dislocation slows down oxide ion diffusion in doped CeO_2 by segregation of charged defects. *Nat. Commun.* **2015**, *6*, 6294. [[CrossRef](#)]
132. Ma, W.; Kim, J.J.; Tsvetkov, N.; Daio, T.; Kuru, Y.; Cai, Z.; Chen, Y.; Sasaki, K.; Tuller, H.L.; Yildiz, B. Vertically aligned nanocomposite $La_{0.8}Sr_{0.2}CoO_3/(La_{0.5}Sr_{0.5})_2CoO_4$ cathodes—Electronic structure, surface chemistry and oxygen reduction kinetics. *J. Mater. Chem. A* **2015**, *3*, 207–219. [[CrossRef](#)]
133. Marrocchelli, D.; Sun, L.; Yildiz, B. Dislocation in $SrTiO_3$: Easy to reduce but not so fast for oxygen transport. *J. Am. Chem. Soc.* **2015**, *137*, 4735–4748. [[CrossRef](#)] [[PubMed](#)]
134. Saranya, A.M.; Morata, A.; Pla, D.; Burriel, M.; Chiabrera, F.; Garbayo, I.; Hornes, A.; Kilner, J.A.; Tarancon, A. Unveiling the outstanding oxygen mass transport properties of Mn-rich perovskites in grain boundary-dominated $La_{0.8}Sr_{0.2}(Mn_{1-x}Co_x)_{0.85}O_{3\pm\delta}$ nanostructures. *Chem. Mater.* **2018**, *30*, 5621–5629. [[PubMed](#)]
135. Lee, D.; Gao, X.; Sun, L.; Jee, Y.; Poplawsky, J.; Farmer, T.O.; Fan, L.; Guo, E.-J.; Lu, Q.; Heller, W.T.; et al. Colossal oxygen vacancy formation at a fluorite-bixbyite interface. *Nat. Commun.* **2021**, *11*, 1371. [[CrossRef](#)]
136. Baiutti, F.; Chiabrera, F.; Acosta, M.; Diercks, D.; Parfitt, D.; Santiso, J.; Wang, X.; Cavallaro, A.; Morata, A.; Wang, H.; et al. A high-entropy manganite in an ordered nanocomposite for long-term application in solid oxide cells. *Nat. Commun.* **2021**, *12*, 2660. [[CrossRef](#)] [[PubMed](#)]
137. Kuganathan, N.; Baiutti, F.; Tarancon, A.; Fleig, J.; Chroneos, A. Defects energetics in the $SrTiO_3$ - $LaCrO_3$ system. *Solid State Ion.* **2021**, *361*, 115570. [[CrossRef](#)]
138. Saravanan, K.; Mason, C.W.; Rudola, A.; Wong, K.H.; Balaya, P. The First Report on Excellent Cycling Stability and Superior Rate Capability of $Na_3V_2(PO_4)_3$ for Sodium Ion Batteries. *Adv. Energy Mater.* **2013**, *3*, 444–450. [[CrossRef](#)]
139. Serras, P.; Palomares, V.; Goñi, A.; Kubiak, P.; Rojo, T. Electrochemical performance of mixed valence $Na_3V_2O_{2x}(PO_4)_2F_{3-2x}/C$ as cathode for sodium-ion batteries. *J. Power Sources* **2013**, *241*, 56–60. [[CrossRef](#)]
140. Sharma, N.; Serras, P.; Palomares, V.; Brand, H.E.A.; Alonso, J.; Kubiak, P.; Fdez-Gubieda, M.L.; Rojo, T. Sodium distribution and reaction mechanisms of a $Na_3V_2O_2(PO_4)_2F$ Electrode during use in a sodium-ion battery. *Chem. Mater.* **2014**, *26*, 3391–3402. [[CrossRef](#)]
141. Bui, K.M.; Dinh, V.A.; Okada, S.; Ohno, T. Hybrid functional study of the NASICON-type $Na_3V_2(PO_4)_3$: Crystal and electronic structures, and polaron-Na vacancy complex diffusion. *Phys. Chem. Chem. Phys.* **2015**, *17*, 30433–30439. [[CrossRef](#)]
142. Li, H.; Peng, L.; Zhu, Y.; Chen, D.; Zhang, X.; Yu, G. An advanced high-energy sodium ion full battery based on nanostructured $Na_2Ti_3O_7/VOPO_4$ layered materials. *Energy Environ. Sci.* **2016**, *9*, 3399–3405. [[CrossRef](#)]
143. Shen, W.; Li, H.; Guo, Z.; Wang, C.; Li, Z.; Xu, Q.; Liu, H.; Wang, Y.; Xia, Y. Double-Nanocarbon Synergistically Modified $Na_3V_2(PO_4)_3$: An Advanced Cathode for High-Rate and Long-Life Sodium-Ion Batteries. *ACS Appl. Mater. Interfaces* **2016**, *8*, 15341–15351. [[CrossRef](#)] [[PubMed](#)]

144. Vellaisamy, M.; Reddy, M.V.; Chowdari, B.V.R.; Kalaiselvi, N. Exploration of AVP₂O₇/C (A = Li, Li_{0.5}Na_{0.5}, and Na) for High-Rate Sodium-Ion Battery Applications. *J. Phys. Chem. C* **2018**, *122*, 24609–24618. [[CrossRef](#)]
145. Jin, T.; Li, H.; Zhu, K.; Wang, P.F.; Liu, P.; Jiao, L. Polyanion-type cathode materials for sodium-ion batteries. *Chem. Soc. Rev.* **2020**, *49*, 2342–2377. [[CrossRef](#)] [[PubMed](#)]
146. Zakharkin, M.V.; Drozhzhin, O.A.; Ryazantsev, S.V.; Chernyshov, D.; Kirsanova, M.A.; Mikheev, I.V.; Pazhetnov, E.M.; Antipov, E.V.; Stevenson, K.J. Electrochemical properties and evolution of the phase transformation behavior in the NASICON-type Na_{3+x}Mn_xV_{2-x}(PO₄)₃ (0 ≤ x ≤ 1) cathodes for Na-ion batteries. *J. Power Sources* **2020**, *470*, 228231. [[CrossRef](#)]
147. Kovrugin, V.M.; Chotard, J.-N.; Fauth, F.; Masquelier, C. Na₇V₃(P₂O₇)₄ as a high voltage electrode material for Na-ion batteries: Crystal structure and mechanism of Na⁺ extraction/insertion by operando X-ray diffraction. *J. Mater. Chem. A* **2020**, *8*, 21110–21121. [[CrossRef](#)]
148. Zhao, D.; Wang, C.; Ding, Y.; Ding, M.; Cao, Y.; Chen, Z. Will Vanadium-Based Electrode Materials Become the Future Choice for Metal-Ion Batteries? *ChemSusChem* **2022**, *15*, e202200479. [[CrossRef](#)]

Disclaimer/Publisher's Note: The statements, opinions and data contained in all publications are solely those of the individual author(s) and contributor(s) and not of MDPI and/or the editor(s). MDPI and/or the editor(s) disclaim responsibility for any injury to people or property resulting from any ideas, methods, instructions or products referred to in the content.